Agromet 38 (2): 68-77, 2024

Agromet
journal.ipb.ac.id/index.php/agromet
ISSN : 0126 - 3633

Identification of Peatland Burned Area based on Multiple Spectral Indices and Adaptive Thresholding in Central Kalimantan

Hilda Ayu Pratikasiwi[1], Muh. Taufik[2], I Putu Santikayasa[2], Dede Dirgahayu Domiri[1]

[1] National Research and Innovation Agency, Indonesia 16915

[2] Department of Geophysics and Meteorology, Faculty of Mathematics and Natural Sciences, IPB University, Dramaga Campus, Bogor, Indonesia 16680

ARTICLE INFO

Received
30 July 2024

Revised
11 September 2024

Accepted for Publication
1 Oktober 2024

Published
3 Oktober 2024

doi: 10.29244/j.agromet.38.2.68-77

Correspondence:
Muh. Taufik
Department of Geophysics and Meteorology, IPB University, Bogor, Indonesia16680
Email: mtaufik@apps.ipb.ac.id

ABSTRACT

Nowadays, spectral index has become popular as a tool to identify fire-burned areas. However, the use of a single index may not be universally applicable to region with diverse landscape and vegetation as peatlands. Here, we propose to develop a procedure that integrates multiple spectral indices with an adaptive thresholding method to enhance the performance of burned area detection. We combined the Normalized Difference Vegetation Index (NDVI) and the Normalized Burn Ratio (NBR) using MODIS imagery from 2002 to 2022 to calculate $dNBR_{CBP}$ (Confirmed Burned Pixel) by filtering dNDVI and dNBR. The mean and standard deviation of $dNBR_{CBP}$ serve as inputs for image thresholding. We tested our approach in Sebangau peatland, Central Kalimantan, where fires occur annually. The results showed that the model performed well with overall accuracy > of 91%, indicating that the model is effective and reliable for identifying burned areas. The findings also revealed that the frequency of fire is below 2 times/year, with the southeastern is the most fire prone regions. Further, our findings provide an alternative approach for identifying burned areas in locations with diverse vegetation cover and different geographical regions.

KEYWORDS

Accuracy, Fire Frequency, Normalized Burn Ratio, Normalized Difference Vegetation Index, Peat Fire

1. INTRODUCTION

Peat fires in Indonesia have increased since 1960 (Field et al., 2009) and become more frequent since 1997 (Hoscilo et al., 2011). A study reported that at least 10–15% of Indonesia's peatlands experience fires annually (Page and Hooijer, 2016), especially for Central Kalimantan, one of the largest peatland areas in Indonesia, where the ex-mega rice project exists. Frequent peat fires have caused detrimental impacts on biodiversity (Agus et al., 2019), hydrology (Taufik et al., 2017), and the environment (Kettridge et al., 2019). Also, fires have transformed pristine peat swamp forests into fire-prone shrubs (Miettinen et al., 2012). During strong El Niño, such as in 2015, mega-fires cost USD 19.1 billion, worsened air quality, and increased adverse health effects (World Bank, 2016).

Identifying burned areas will benefit from assessing the extent of fire damage (Hoscilo et al., 2011), which is mainly evaluated at field level or using satellite data (Alcaras et al., 2022). There are typically two approaches for satellite data evaluation: classification methods and spectral indices (Woźniak and Aleksandrowicz, 2019). There are numerous classifications of burned area, including supervised classification (Sirin and Medvedeva, 2022), image thresholding, object-based approaches (Milczarek et al., 2023), and fuzzy set theory (Nebot and Mugica, 2021).

On the other hand, spectral indices (SIs) combine various spectral bands, which are used to distinguish between pre-fire and post-fire images and effectively identify burned and unburned areas (Woźniak and Aleksandrowicz, 2019).

Despite their widespread use in burned area mapping, identifying the most suitable SIs remains challenging due to the variability in their performance across different conditions. Some studies evaluate burned areas using a single spectral index for the summer season without assessing the effectiveness under diverse environmental conditions (Bastarrika et al., 2011; Smiraglia et al., 2020; Stroppiana et al., 2012). Since the spectral response is influenced by atmospheric conditions, satellite characteristics, and local site conditions, a single SI may not be universally applicable (Fornacca et al., 2018; Stroppiana et al., 2012). Therefore, integrating multiple SIs can leverage the strengths of different spectral band combinations, enhancing the accuracy and reliability of burned area detection across varied conditions. This research combines multiple spectral indices to improve burned area detection methods, such as the Normalized Difference Vegetation Index (NDVI) and the Normalized Burn Ratio (NBR).

NDVI is a vegetation index that is particularly effective in differentiating between burned and unburned areas due to its intense sensitivity to vegetation changes (Chen et al., 2011; Pang et al., 2017). Fire alters the surface reflectance by reducing near-infrared reflectance and increasing red reflectance due to vegetation loss, leading to notable changes in NDVI value (Tiwari et al., 2024). NDVI is highly sensitive to vegetation greenness, giving an effective index for distinguishing the potential photosynthetic capacity of trees affected by fires (Pompa-García et al., 2022). On the other hand, NBR is a widely recognized index for detecting burned areas (Spracklen and Spracklen, 2023; Vetrita et al., 2021) as it best separates burned areas from shadows and water bodies (Stroppiana et al., 2012). Combining NDVI and NBR will improve the detection of burned areas and distinguish more accurately between burned vegetation and other land cover types.

Studies on burned areas have combined SIs and adaptive thresholding (Smiraglia et al., 2020; Woźniak and Aleksandrowicz, 2019) with some adjustments to adapt to landscape conditions. Adaptive thresholding addresses the variability in spectral responses to burning across different biomes (Boschetti et al., 2015). This threshold improved the fixed threshold method that often fails to account for the diverse ecological parameters and spectral sensitivity associated with various regions, leading to inconsistent results (Kolden et al., 2015). Smiraglia et al., (2020) expanded on using adaptive thresholding by integrating the agreement index and spectral indices for burned area classification in temperate regions.

Here, we test the adaptive image thresholding for humid tropical peatland area in Indonesia. The area is characterized by highly variable moisture content (Taufik et al., 2022) and a mix of dense and sparse vegetation (Miettinen et al., 2012), which significantly affect the spectral responses used in burned area detection. Here, we aim to combine spectral indices that consider vegetation changes, such as NDVI and NBR, with adaptive thresholding techniques to better capture the diverse characteristics of peatland fires without using regression-based thresholds. The specific objectives are: (i) to propose an integration of multiple spectral indices and adaptive images thresholding to detect burned areas, (ii) to evaluate the classification accuracy of adaptive image thresholding, and (iii) to calculate the annual fire frequency in the study site. Our methodology will provide an alternative method for identifying burned areas in locations with diverse vegetation cover and different geographical regions in Indonesian peatland.

2. RESEARCH METHODS

2.1 Study Site and Data Source

The research site is on the Kahayan – Sebangau Peatland Hydrological Unit (PHU) in Pulang Pisau Regency, Central Kalimantan, Indonesia. The PHU covers approximately 0.45 Mha of peatland (Cahyono et al., 2022). The climate is characterized by strong monsoons (Aldrian and Susanto, 2003), with a peak dry season in July-September (Usup and Hayasaka, 2023). The annual rainfall is above 2000 mm (Hirano et al., 2015), slightly lower than other tropical peatlands in Indonesia (Taufik et al., 2023). Climate-induced drought is associated with the El Niño events and contributes to frequent fires.

We used Modis-Terra data (MOD09A1), provided by Land Processes Distributed Active Archive Center, from 2002-2022 with a spatial resolution of 500 m (https://lpdaac.usgs.gov/products/mod09a1v061/), to calculate burn area and fire occurrence. Modis MOD09A1 was derived from the best observations of Terra over 8-day periods, as assessed by observational coverage and overall pixel quality. The surface spectral reflectance for each band has been measured at ground level and has atmospheric corrections for gases, aerosols, and Rayleigh scattering (Vermote, 2021). MOD09A1 provided 13 bands, but we only selected Bands 1 - 7 for this study to separate burned and unburned areas. Specifically, Bands 6 (1628–1652 nm) and 7 (2105–2155 nm) are the Shortwave Infrared

(SWIR) bands, which are sensitive to variations in moisture content and are instrumental in identifying post-fire changes. Bands 2 (841–876 nm) and 3 (459–479 nm) correspond to the Near Infrared (NIR), and Red bands are essential for evaluating vegetation health and detecting fire impact. These bands will be used to calculate vegetation indices such as the NBR and the NDVI. We also used reference data from the Indonesian Ministry of Environment and Forestry to validate the predicted burn area (https://sipongi.menlhk.go.id/).

2.2 Normalized Burn Ratio (NBR)

NBR index uses NIR and SWIR wavelengths, where high NBR values generally indicate healthy vegetation, while low values indicate bare land and burned areas (Alcaras et al., 2022). In healthy vegetation, NIR reflectance is typically high due to the internal structure of plant cells, which strongly reflect NIR light. Burned areas show relatively low reflectivity in the NIR band and a high reflectance in the SWIR band. Due to their inherent physical properties, water bodies and shadows have low reflectance in both the NIR and SWIR bands. However, unlike burned areas, they do not show a characteristic increase in SWIR reflectance (Duan et al., 2024). The NBR is formulated in Equation 1.

$$\mathrm{NBR} = \frac{\mathrm{R_{NIR}} - \mathrm{R_{SWIR}}}{\mathrm{R_{NIR}} + \mathrm{R_{SWIR}}} \quad (1)$$

where $\mathrm{R_{NIR}}$ is a NIR reflectance (Modis band 2) and $\mathrm{R_{SWIR}}$ is a Short Wave Infrared (SWIR) reflectance (Modis band 6).

NBR value was calculated from pre-fire and post-fire occurrence to determine the extent and severity of vegetation change caused by fire (Key and Benson, 2006). Pre-fire and post-fire NBR values were taken from satellite imagery for each month, assuming that the duration of the fires was one month. The fire duration varies depending on weather conditions and fire management practices (Konecny et al., 2016). We selected a one-month interval to consistently monitor vegetation changes affected by fire, which is suitable for monthly temporal analysis. This approach ensures a clear distinction between fire events and minimizes the risk of duplication when calculating fire occurrences at the exact location or pixel. The one-month interval also helps to reduce the impact of cloud cover by allowing for the selection of clearer satellite imagery.

Pre-fire images were selected from MODIS satellite images at the end of the previous month, while post-fire images were obtained from composite satellite images in the current month. High NBR values indicate healthy vegetation, while low NBR values indicate bare soil and burned areas. When a fire occurs, vegetation is damaged, and the NBR value decreases from the original value. The size of the burned area was assessed as the difference between the pre-fire and post-fire NBR, which is called dNBR (Equation 2).

$$\mathrm{NBR} = \mathrm{NBR_{prefire}} - \mathrm{NBR_{postfire}} \quad (2)$$

2.3 Normalized Difference Vegetation Index (NDVI)

NDVI is generally used to assess the greenness of vegetation. NDVI measures the ratio value between the NIR bands reflected by vegetation and the RED bands absorbed by vegetation. Healthy vegetation reflects more NIR waves and absorbs RED waves. NDVI values range from −1 to +1, where positive values indicate a higher vegetation index and negative values indicate a lower one (Equation 3).

$$\mathrm{NDVI} = \frac{\mathrm{R_{NIR}} - \mathrm{R_{Red}}}{\mathrm{R_{NIR}} + \mathrm{R_{Red}}} \quad (3)$$

where $\mathrm{R_{Red}}$ is the Red reflectance (Modis Band 1).

When a fire occurs, NDVI value decreases due to a loss of greenness as a decrease in NIR reflectance (Tiwari et al., 2024). NDVI value after fire was lower than the previous NDVI value. The difference in NDVI values before and after a fire can be determined using dNDVI, as shown in Equation 4.

$$\mathrm{dNDVI} = \mathrm{NDVI_{postfire}} - \mathrm{NDVI_{prefire}} \quad (4)$$

$\mathrm{NDVI_{postfire}}$ represences NDVI value after the fire, and $\mathrm{NDVI_{prefire}}$ is NDVI value before the fire. A positive dNDVI indicates vegetation growth or a process of ecological recovery within the region, especially after fire incidents or land degradation. A negative dNDVI reflects decreased vegetation cover, likely from wildfires or other ecological disturbances.

2.4 Burn Area Detection

Burned areas and non-burned areas in this study were identified by changes in vegetation reflectance values using NBR, NDVI, and adaptive thresholding (Fraser et al., 2000). Using Equation 5, we combined the dNBR and dNDVI values to form the Confirmed Burned Pixel (CPB).

$$\mathrm{dNBR_{CBP}} = \mathrm{dNBR}, \mathrm{if} \begin{cases} \mathrm{dNBR} > 0 \\ \mathrm{dNDVI} < 0 \end{cases} \quad (5)$$

where $\mathrm{dNBR_{CBP}}$ is the dNBR Confirmed Burned Pixel (CBP) value, filtered according to equation 5, while values other than that are considered null. The $\mathrm{dNBR_{CBP}}$ value would determine the separated Burn Area (BA) threshold.

The thresholds were determined by analyzing each pixel group's index values yearly based on their mean and standard deviation (stdev) of CPB (Equation 6). For each month, we selected pixels with a dNBR increase greater than +1 stdev from the mean $\mathrm{dNBR_{CBP}}$. We choose the +1 standard deviation (stdev) threshold for dNBR calculation because it provides more reliable

and adaptive threshold for identifying burned areas across a wide range of landscapes. A study revealed that the +1 stdev threshold effectively captured most of the burned pixels (Fraser et al., 2000), ensuring that almost all fire-affected areas were detected. Using only the mean would be too conservative, potentially missing subtle burn signals, especially in regions with diverse vegetation responses to fire.

Standard deviation incorporates the natural variation in vegetation response, allowing for a more regionally adaptive threshold to account for different levels of fire impact across various vegetation types. This made +1 stdev for dNBR have a balanced approach compared to the extremes of other thresholds (i.e. +2, -2, -1), which either include too few or too many false positives. Additionally, the post-fire NBR values need to be lower than -1 stdev to ensure that significant changes in vegetation after the fire are accurately detected. This approach discerns the variability among the groups, facilitating the application of these findings to other fire events.

$$\mathrm{BA} = \mathrm{dNBR} > (\mu + \sigma)_{\mathrm{dNBR_{CPB}}}$$
$$\text{and } \mathrm{NBR_{postfire}} < (\mu - \sigma)_{\mathrm{dNBR_{CPB}}} \quad (6)$$

where BA is the burned area, μ is the average value of $dNBR_{CBP}$ while σ is the standard deviation.

2.5 Accuracy Assessment

Accuracy assessment is an essential step in evaluating the model's performance in fire detection. We applied a confusion matrix by comparing each pixel of the unburned and burned pixel model with ground-based fire data from the Indonesian Ministry of Environment and Forestry. We limited our ground based fire data selection to 2013 to 2022 due to the only availability of comprehensive fire detection records within this timeframe. The confusion matrix is a multidimensional table with cells representing variations in one class over, which included Ommision Error (OE), Commision Error (CE), the accuracies of the Producer (PA), User (UA), and Overall (OA).

In addition to overall accuracy, we evaluated omission errors (producer accuracy) and commission errors (user accuracy) to address the imbalanced class distribution. We assessed the model performance by calculating the proportion of user and producer accuracies exceeding thresholds of 70%. We categorized classification performance as follows: 'very good' for accuracies >90%, 'good' for accuracies between 80% and 90%, 'acceptable' for accuracies between 70% and 80%, and 'unacceptable' for accuracies <70% (Woźniak and Aleksandrowicz, 2019). The model was classified as effective and reliable if the overall accuracy exceeded 90%. We processed the data and statistical analysis using R language (R Core Team, 2021).

3. RESULTS

3.1 Burn Area Threshold

Figure 1 presents the boxplot of burned area thresholds (mean +1 stdev) from 2002 to 2022, highlighting the variability of the monthly thresholds over the years. Adaptive thresholding adjusts the threshold values based on monthly data, ensuring that the detection of burned areas is responsive to changes in environmental conditions and fire characteristics over time. Each burned area is indicated by $dNBR_{CBP}$ (delta Normalised Burn Ratio Confirmed Burned Pixels)

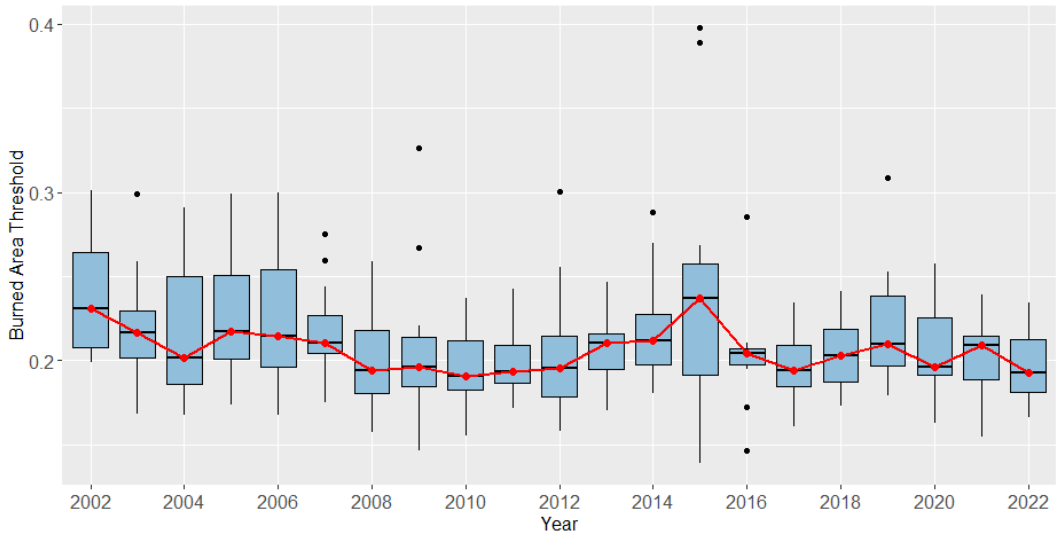

Figure 1. Delta Normalized Burn Ratio (dNBR) threshold value (mean +1 stdev) from 2002-2022. The boxes point out the median, and the 25% and 75% quantiles for each year data. The whiskers represent 10 and 90% of quantiles. The dots indicate outliers. The red line is the median value of yearly thresholds.

threshold value.

Figure 1 provides a threshold value used to detect burned areas over two decades (2002-2022), revealing significant fluctuations. Each box represents the interquartile range of the monthly thresholds for a given year, with the line extending to the minimum and maximum values, excluding outliers. The presence of outliers, particularly in years like 2015, indicates extreme fire activities that corresponds with higher threshold values, where increases in dNBR thresholds reflect the intensity of these fire events.

The line splitting the box in two represents the median value of the monthly threshold in that year. The median threshold value typically ranges from 0.1 to 0.3, with an average all threshold of approximately 0.21. Notably, the highest thresholds were observed in 2015 around 0.24. The thresholds from 2011 to 2022 showed a more stable trend with fewer extreme outliers, indicating a relatively consistent approach in detecting burned areas during this period.

3.2 Burn Area Accuracy Assessment

Table 1 presents the accuracy assessment of burned area detection in Kahayan Sebangau peatland from 2013 to 2022. The evaluation metrics include overall accuracy (OA), producer's accuracy (PA), user's accuracy (UA), omission error (OE), and commission error (CE). The analysis reveals a generally high overall accuracy of burned area detection, with an average of 90%. However, there are notable variations across the years. The highest OA was achieved in 2022 at 98%, while the lowest occurred in 2015 at 78%. The model can be classified as effective and reliable, with an overall accuracy exceeding 90%.

The model exhibits a consistent performance across years, with both producer and user accuracies exceeding the 70% threshold. Both omission and commission errors were relatively low. Omission errors, which indicate the model's failure to detect actual burned areas, have averaged 10%. The highest omission error of 20% occurred in 2015, coinciding with the year with the lowest overall accuracy. Commission errors, representing the model's incorrect identification of unburned areas as burned, were consistently low at an average of 2%. This indicates the model's effectiveness in correctly identifying burned areas while reducing false positives (classifying unburned areas as burned) and false negatives (missing actual burned areas).

Commission and omission errors were also evaluated to understand the model's reliability better. We showed the spatial distribution of commission and omission errors for two significant fire years, 2015 and 2019, which were strongly influenced by El Niño events. Figure 2 illustrates the spatial distribution of burned and unburned areas and omission and commission errors for 2015 and 2019. The omission error for 2015 was 20%, indicating that the model missed a significant portion of burned areas, particularly in the central and southern portions. Commission errors (green), representing unburned areas mistakenly classified as burned, occurred at a rate of 6%, suggesting some overestimation in certain areas.

Table 1. The Model accuracy of burned area detection in Kahayan Sebangau peatland from 2013 - 2022. The overall accuracy (OA), producer's accuracy (PA), user accuracy (UA), omission error (OE), and commission error (CE) are estimated for all fires that happened in each year.

Year	Overall Accuracy (%)	Producer's accuracy (%)	Omission Error (%)	User's Accuracy (%)	Commission Error (%)
2013	93	93	7	99	1
2014	83	84	16	99	1
2015	78	80	20	94	6
2016	88	88	12	99	1
2017	93	92	8	99	1
2018	87	88	12	99	1
2019	84	85	15	97	3
2020	94	94	6	99	1
2021	97	97	3	99	1
2022	98	98	2	99	1
Average	90	90	10	98	2

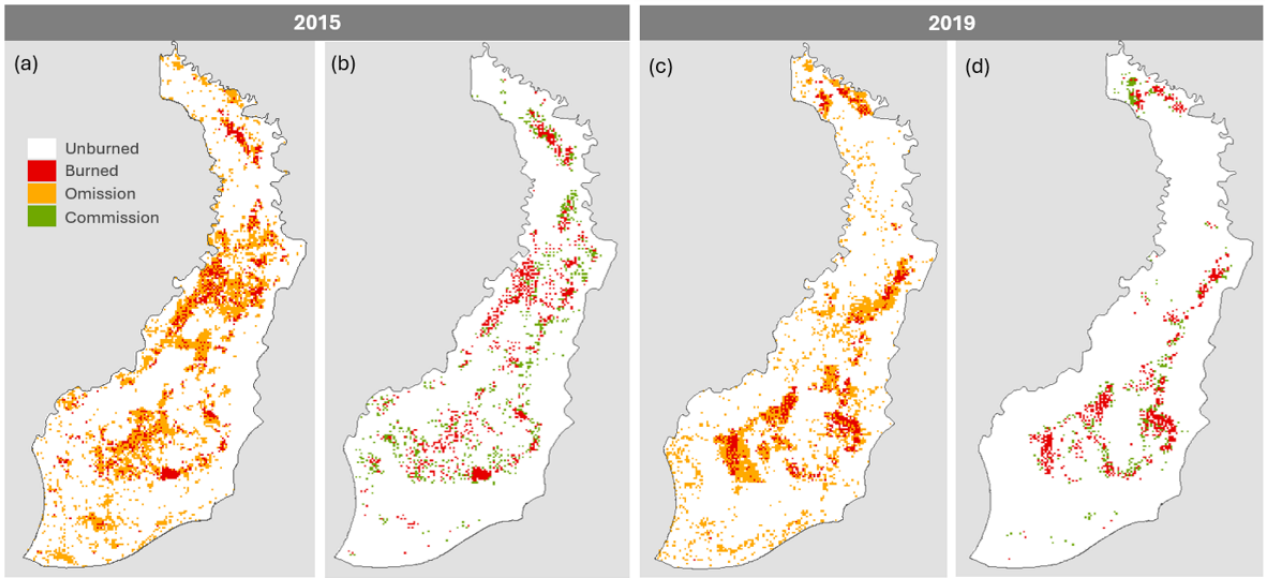

Figure 2. Maps of burned and unburned areas for 2015 and 2019 with (a) ommision errors for 2015, (b) commission errors for 2015, (c) ommision errors for 2019, and (d) commission errors for 2019.

The spatial distribution of the burned areas in 2019 (Figures 2c and 2d) revealed a lower density of burned areas and fewer omission and commission errors overall. The omission error in 2019 was 15%, reflecting improved detection but still missing some burned areas, particularly in central regions. Commission errors in 2019 dropped to 3%, indicating a more accurate classification of unburned areas compared to 2015.

3.3 Fire Frequency based on Spectral Indices and Adaptive Thresholding

The presented model demonstrates a robust method for calculating fire frequency in the Kahayan Sebangau PHU. By analyzing burn areas annually from 2002 to 2022, we can observe the spatial and temporal patterns of fires in this region. Figure 3 presents the spatial distribution of annual fire frequency in the Kahayan Sebangau PHU. The range of fire occurrence is from 1 to 8 events per year, with most regions experiencing no fire to two fire events each year.

The annual burn area maps provide a detailed visual representation of how fire activity fluctuates over time within the region. Figure 3 shows the fluctuating fire frequencies between 2002 and 2015, followed by a decreasing fire frequency and burn area trend from 2016 to 2022. From 2003 to 2005, there was a noticeable increase in fire occurrences, particularly in the northern part, as indicated by the transition from green to yellow areas. In 2009, fire activity was more dispersed, with a notable cluster in the north of the region, while 2011 and 2012 show a marked decrease in fire frequency across most areas. The period from 2013 to 2014 reflects a moderate level of fire activity with scattered distributions. However, 2015 stands out with a significant surge in fire frequency, again concentrated in the central and northern parts.

The 2016 and 2020 fire activity levels displayed relatively low compared to previous years. However, 2019 shows a noticeable increase in burn areas, indicating a resurgence of fire activity. Years of 2021 and 2022 again show lower burn areas, suggesting a return to less frequent fires. For 2002, 2006, and 2015, fire frequency was greater than once per year, with significant concentration around the central and northern parts of the region. This data reveals fluctuations in fire occurrences over the years, emphasizing the need for continuous monitoring to understand and manage fire risks in the Kahayan Sebangau.

4. DISCUSSION

The fire frequency in the Kahayan Sebangau region has varied throughout the years. The annual burn area maps reveal that specific years exhibit higher fire activities than others. The area and fire frequency have increased significantly in 2002, 2006, 2015, and 2019. The increase can be linked to the El Niño events, which cause extreme dry conditions, exacerbating fire occurrences in Kalimantan, Indonesia. El Niño is characterized by reduced rainfall and lower soil moisture levels, rendering the soil and vegetation more susceptible to fires (Taufik et al., 2022).

Fire frequency in the Kahayan Sebangau peatland typically ranges from 0 to 2 events per year, but some pixels show more frequent fires, up to 8 times per year(Figure 3). This high occurrence in specific pixels may result from the NBR monthly pre-fire and post-fire

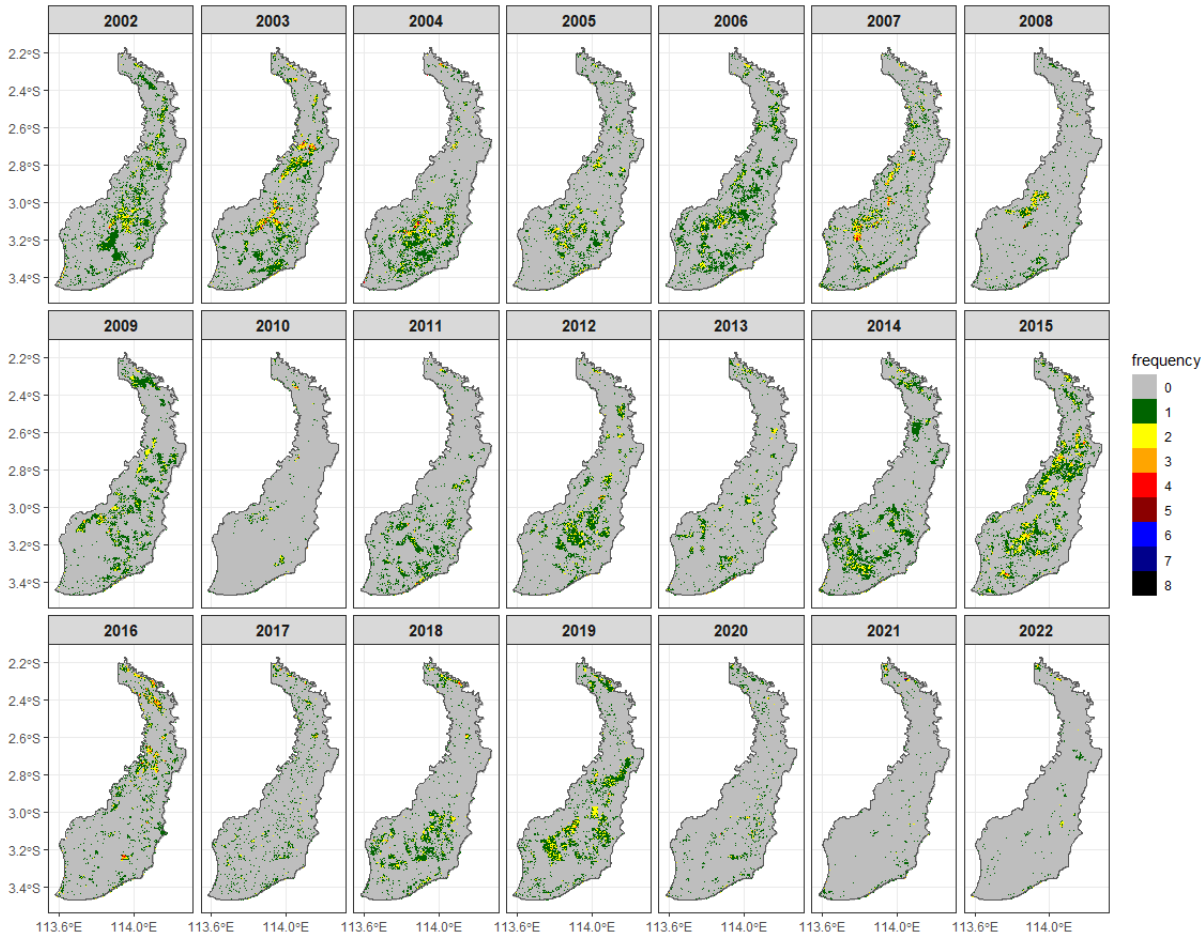

Figure 3. Spatial distribution of annual fire frequency in the Kahayan Sebangau PHU from 2002-2022.

date calculations. Since the model uses monthly data, fires that start in one month and continue into the next month are counted as separate events. Fire significantly increases in dry vegetation, particularly in degraded shrublands (Taufik et al., 2024), especially in non-managed regions (lowered part of Figure 3) like the drained peatlands of the former Mega Rice Project (Vetrita and Cochrane, 2019). These environments, with their low moisture content and flammable plant material, are particularly susceptible to ignition and rapid fire spread.

The proposed procedure first integrated two SIs to be used as a reference, then calculates thresholds from those SIs, and computes a single burned area mask. A single spectral index is usually used to assess burned areas in specific conditions (Bastarrika et al., 2011; Smiraglia et al., 2020; Stroppiana et al., 2012), which may not applicable for diverse landscape such as PHU Sebangau. Our study demonstrated the advantages of integrating multiple spectral indices, such as NBR and NDVI, along with adaptive thresholding to enhance burned area detection (Figure 1). Further, we confirmed the similar findings that visible and near-infrared domains are more suitable for immediate post-fire assessment (Chen et al., 2011; Fornacca et al., 2018).

In addition, previous studies applied a single threshold approach when analyzing burn severity for specific times. For example, a dNBR threshold below 0.053 was used to classify unburned areas in Kalimantan peatland (Hoscilo et al., 2011; Schmidt et al., 2024). In Boreal Forest Alaska, a threshold of 0.085 was applied to differentiate burned-unburned classification (Epting and Verbyla, 2005). Our threshold value is closed to the threshold low severity class for tropical forests in Kalimantan (Hoscilo et al., 2011). However, the threshold, which is based on a single image or time, often fall within a narrow range, making them unsuitable for capturing the ecological and vegetation changes observed over time. The adaptive thresholding approach presented in this study offers dynamic and adaptable detection thresholds for burned areas with a good performance (Table 1), particularly in Kalimantan's diverse and ecologically variable regions.

Future research should prioritize the development of more detailed methods for identifying pre- and post-fire dates to enhance the accuracy of fire frequency estimates. The current assumption of a one-month fire duration may need to be revised to capture the complex dynamics of peatland fires. Accurate pre-fire and post-fire date estimations are crucial for

understanding the temporal patterns of fire activity and evaluating the effectiveness of restoration efforts.

In Indonesia, the Peatland Restoration Agency (Badan Restorasi Gambut, BRG) has implemented rewetting programs to restore the natural hydrology of degraded peatlands, including the Kahayan Sebangau region. These efforts have focused on minimizing drainage and maintaining appropriate water table levels to preserve hydrological and ecological functions (Yuwati et al., 2021). The implementation of rewetting has significantly reduced fire areas and the number of fire events (Taufik et al., 2023). Identifying precise fire and post-fire dates is particularly important in rewetting activities. By accurately determining the timing of fires, researchers can better assess the effectiveness of rewetting in preventing recurring fires and evaluating the long-term impacts of restoration efforts on peatland ecosystems.

The combination of NBR and NDVI to observe vegetation changes before and after a fire is quite effective in detecting fire occurrences, consistent with other research to use NBR (Sirin and Medvedeva, 2022) and NDVI (Rendana et al., 2023) for peat fire detection. However, futher study is needed to identify the most suitable spectral indices in peatland ecosystems before considering the combination of multiple spectral. A comprehensive evaluation of various indices will enhance the accuracy and reliability of burn area detection in these unique environments. It is crucial to select the highest-performing spectral indices (SIs), which may depend on vegetative status, and to integrate them to achieve the most precise mapping, balancing omission and commission errors and optimizing overall accuracy (Smiraglia et al., 2020).

Our research used adaptive thresholding, which dynamically adjusts based on varying ecological conditions and temporal factors. Unlike single threshold methods, which may have limitations in diverse or changing environments, adaptive thresholding can better accommodate environmental conditions and seasonal changes, potentially reducing omission and commission errors (Smiraglia et al., 2020). This adaptability is particularly advantageous in peatland ecosystems, characterized by their dynamic nature and susceptibility to disturbances. However, it is important to note that adaptive thresholding may have limitations. For example, the effectiveness of adaptive thresholding depends on the quality, quantity, and variability of the data used to calculate the model. Additionally, this method may struggle with extreme values, as it relies on statistical estimates of the mean and standard deviation to determine the threshold for burned areas, which can be skewed by outliers or extreme fire activity.

5. CONCLUSIONS

This paper proposes a method for detecting burned areas in diverse peatland ecosystems by combining multiple spectral indices with adaptive image thresholding. Spectral Indices like The Normalized Difference Vegetation Index (NDVI) and the Normalized Burn Ratio (NBR) are utilized to calculate adaptive thresholds annually. The models demonstrate the mean of overall accuracies over 90% and perform robust classifications to detect burned and unburned pixels effectively. Furthermore, it is shown that multiple spectral indices and the adaptive thresholding technique give more flexible classification in the areas with different conditions like peatland. The models calculate the frequency of fires in the area, showing that most fire occurrences range from 0 to 2 times/year, and some pixels exhibit more than two fires annually. This adaptable methodology enhances the precision and applicability of burn area detection in various land cover types and region characteristics, providing a valuable tool for environmental monitoring and fire impact assessment.

ACKNOWLEDGEMENT

The authors thank LPDP (Indonesia Endowment Fund for Education of Ministry of Finance) for funding this research. We also appreciate the anonymous reviewers and editors for their insightful comments and constructive suggestions, which significantly enhanced the quality of this manuscript. M Taufik was supported by the RIIM LPDP Grant and BRIN, grant number: 106/IV/KS/11/2023.

REFERENCES

Agus, C., Azmi, F.F., Widiyatno, Ilfana, Z.R., Wulandari, D., Rachmanadi, D., Harun, M.K., Yuwati, T.W., 2019. The Impact of Forest Fire on the Biodiversity and the Soil Characteristics of Tropical Peatland, in: Leal Filho, W., Barbir, J., Preziosi, R. (Eds.), Handbook of Climate Change and Biodiversity, Climate Change Management. Springer International Publishing, Cham, pp. 287–303. https://doi.org/10.1007/978-3-319-98681-4_18.

Alcaras, E., Costantino, D., Guastaferro, F., Parente, C., Pepe, M., 2022. Normalized Burn Ratio Plus (NBR+): a new index for Sentinel-2 imagery. Remote Sens. 14, 1727.

Aldrian, E., Susanto, R.D., 2003. Identification of three dominant rainfall regions within Indonesia and their relationship to sea surface temperature. Int. J. Climatol. 23, 1435–1452. https://doi.org/10.1002/joc.950.

Bastarrika, A., Chuvieco, E., Martín, M.P., 2011. Mapping

burned areas from Landsat TM/ETM+ data with a two-phase algorithm: Balancing omission and commission errors. Remote Sens. Environ. 115, 1003–1012.

Boschetti, L., Roy, D.P., Justice, C.O., Humber, M.L., 2015. MODIS–Landsat fusion for large area 30 m burned area mapping. Remote Sens. Environ. 161, 27–42. https://doi.org/10.1016/j.rse.2015.01.022.

Cahyono, B.K., Aditya, T., Istarno, 2022. The Determination of Priority Areas for the Restoration of Degraded Tropical Peatland Using Hydrological, Topographical, and Remote Sensing Approaches. Land 11. https://doi.org/10.3390/land11071094.

Chen, X., Vogelmann, J.E., Rollins, M., Ohlen, D., Key, C.H., Yang, L., Huang, C., Shi, H., 2011. Detecting post-fire burn severity and vegetation recovery using multitemporal remote sensing spectral indices and field-collected composite burn index data in a ponderosa pine forest. Int. J. Remote Sens. 32, 7905–7927. https://doi.org/10.1080/01431161.2010.524678.

Duan, Q., Liu, R., Chen, J., Wei, X., Liu, Y., Zou, X., 2024. Burned area detection from a single satellite image using an adaptive thresholds algorithm. Int. J. Digit. Earth 17. https://doi.org/10.1080/17538947.2024.2376275.

Epting, J., Verbyla, D., 2005. Landscape-level interactions of prefire vegetation, burn severity, and postfire vegetation over a 16-year period in interior Alaska. Can. J. For. Res. 35, 1367–1377. https://doi.org/10.1139/x05-060.

Field, R.D., van der Werf, G.R., Shen, S.S.P., 2009. Human amplification of drought-induced biomass burning in Indonesia since 1960. Nat. Geosci. 2, 185–188. https://doi.org/10.1038/ngeo443.

Fornacca, D., Ren, G., Xiao, W., 2018. Evaluating the best spectral indices for the detection of burn scars at several post-fire dates in a mountainous region of Northwest Yunnan, China. Remote Sens. 10, 1196.

Fraser, R.H., Li, Z., Cihlar, J., 2000. Hotspot and NDVI Differencing Synergy (HANDS): A New Technique for Burned Area Mapping over Boreal Forest. Remote Sens. Environ. 74, 362–376. https://doi.org/10.1016/S0034-4257(00)00078-X.

Hirano, T., Kusin, K., Limin, S., Osaki, M., 2015. Evapotranspiration of tropical peat swamp forests. Glob. Change Biol. 21, 1914–1927. https://doi.org/10.1111/gcb.12653.

Hoscilo, A., Page, S.E., Tansey, K.J., Rieley, J.O., 2011. Effect of repeated fires on land-cover change on peatland in southern Central Kalimantan, Indonesia, from 1973 to 2005. Int. J. Wildland Fire 20, 578. https://doi.org/10.1071/WF10029.

Kettridge, N., Lukenbach, M.C., Hokanson, K.J., Devito, K.J., Petrone, R.M., Mendoza, C.A., Waddington, J.M., 2019. Severe wildfire exposes remnant peat carbon stocks to increased post-fire drying. Sci. Rep. 9, 1–6.

Key, C.H., Benson, N.C., 2006. Landscape Assessment: Ground measure of severity, the Composite Burn Index; and Remote sensing of severity, the Normalized Burn Ratio, in: Lutes, D.C., Keane, R.E., Caratti, J.F.K., C.H., Benson, N.C., Sutherland, S., Gangi, L.J. (Eds.), FIREMON: Fire Effects Monitoring and Inventory System. USDA Forest Service, Rocky Mountain Research Station, Gen. Tech. Rep., Ogden, UT.

Kolden, C.A., Smith, A.M.S., Abatzoglou, J.T., 2015. Limitations and utilisation of Monitoring Trends in Burn Severity products for assessing wildfire severity in the USA. Int. J. Wildland Fire 24, 1023–1028. https://doi.org/10.1071/WF15082.

Konecny, K., Ballhorn, U., Navratil, P., Jubanski, J., Page, S.E., Tansey, K., Hooijer, A., Vernimmen, R., Siegert, F., 2016. Variable carbon losses from recurrent fires in drained tropical peatlands. Glob. Change Biol. 22, 1469–1480. https://doi.org/10.1111/gcb.13186.

Miettinen, J., Shi, C., Liew, S.C., 2012. Two decades of destruction in Southeast Asia's peat swamp forests. Front. Ecol. Environ. 10, 124–128. https://doi.org/10.1890/100236.

Milczarek, M., Aleksandrowicz, S., Kita, A., Chadoulis, R.-T., Manakos, I., Woźniak, E., 2023. Object- Versus Pixel-Based Unsupervised Fire Burn Scar Mapping under Different Biogeographical Conditions in Europe. Land 12, 1087. https://doi.org/10.3390/land12051087.

Nebot, À., Mugica, F., 2021. Forest Fire Forecasting Using Fuzzy Logic Models. Forests 12, 1005. https://doi.org/10.3390/f12081005.

Page, S.E., Hooijer, A., 2016. In the line of fire: the peatlands of Southeast Asia. Philos. Trans. R. Soc. B Biol. Sci. 371, 20150176. https://doi.org/10.1098/rstb.2015.0176.

Pang, G., Wang, X., Yang, M., 2017. Using the NDVI to identify variations in, and responses of, vegetation to climate change on the Tibetan Plateau from 1982 to 2012. Quat. Int., Third Pole: The Last 20,000 Years - Part 2 444, 87–96. https://doi.org/10.1016/j.quaint.2016.08.038.

Pompa-García, M., Martínez-Rivas, J.A., Valdez-Cepeda, R.D., Aguirre-Salado, C.A., Rodríguez-Trejo, D.A., Miranda-Aragón, L., Rodríguez-Flores, F. de J., Vega-Nieva, D.J., 2022. NDVI Values Suggest Immediate Responses to Fire in an Uneven-Aged Mixed Forest Stand. Forests 13, 1901 . https://doi

.org/10.3390/f13111901.

R Core Team., 2021. R: A language and environment for statistical computing. R Foundation for Statistical Computing, Vienna, Austria.

Rendana, M., Idris, W.M.R., Rahim, S.A., Abdo, H.G., Almohamad, H., Al Dughairi, A.A., Albanai, J.A., 2023. Current and future land fire risk mapping in the southern region of Sumatra, Indonesia, using CMIP6 data and GIS analysis. SN Appl. Sci. 5, 210. https://doi.org/10.1007/s42452-023-05432-6.

Schmidt, A., Ellsworth, L.M., Boisen, G.A., Novita, N., Malik, A., Gangga, A., Albar, I., Dwi Nurhayati, A., Putra Ritonga, R., Asyhari, A., Kauffman, J.B., 2024. Fire frequency, intensity, and burn severity in Kalimantan's threatened Peatland areas over two Decades. Front. For. Glob. Change 7. https://doi.org/10.3389/ffgc.2024.1221797.

Sirin, A., Medvedeva, M., 2022. Remote Sensing Mapping of Peat-Fire-Burnt Areas: Identification among Other Wildfires. Remote Sens. 14, 194. https://doi.org/10.3390/rs14010194.

Smiraglia, D., Filipponi, F., Mandrone, S., Tornato, A., Taramelli, A., 2020. Agreement Index for Burned Area Mapping: Integration of Multiple Spectral Indices Using Sentinel-2 Satellite Images. Remote Sens. 12, 1862. https://doi.org/10.3390/rs12111862.

Spracklen, B.D., Spracklen, D.V., 2023. Assessment of peatland burning in Scotland during 1985–2022 using Landsat imagery. Ecol. Solut. Evid. 4, e12296. https://doi.org/10.1002/2688-8319.12296.

Stroppiana, D., Bordogna, G., Carrara, P., Boschetti, M., Boschetti, L., Brivio, P.A., 2012. A method for extracting burned areas from Landsat TM/ETM+ images by soft aggregation of multiple Spectral Indices and a region growing algorithm. ISPRS J. Photogramm. Remote Sens. 69, 88–102.

Taufik, M., Haikal, M., Widyastuti, M.T., Arif, C., Santikayasa, I.P., 2023. The Impact of Rewetting Peatland on Fire Hazard in Riau, Indonesia. Sustainability 15, 2169. https://doi.org/10.3390/su15032169.

Taufik, M., Santikaysa, I.P., Haikal, M., Widyastuti, M.T., Arif, C., 2024. Dataset of physical properties of histosols topsoils effected by wildfire in Indonesia. Data Brief 53, 110257. https://doi.org/10.1016/j.dib.2024.110257.

Taufik, M., Torfs, P.J.J.F., Uijlenhoet, R., Jones, P.D., Murdiyarso, D., Van Lanen, H.A.J., 2017. Amplification of wildfire area burnt by hydrological drought in the humid tropics. Nat. Clim. Change 7, 428–431. https://doi.org/10.1038/nclimate3280.

Taufik, M., Widyastuti, M.T., Sulaiman, A., Murdiyarso, D., Santikayasa, I.P., Minasny, B., 2022. An improved drought-fire assessment for managing fire risks in tropical peatlands. Agric. For. Meteorol. 312, 108738. https://doi.org/10.1016/j.agrformet.2021.108738.

Tiwari, A., Nanjundan, P., Kumar, R.R., Soni, V.K., 2024. A framework for natural resource management with geospatial machine learning: a case study of the 2021 Almora forest fires. Fire Ecol. 20, 78. https://doi.org/10.1186/s42408-024-00293-9.

Usup, A., Hayasaka, H., 2023. Peatland Fire Weather Conditions in Central Kalimantan, Indonesia. Fire 6, 182. https://doi.org/10.3390/fire6050182.

Vermote, E., 2021. MODIS/Terra Surface Reflectance 8-Day L3 Global 500m SIN Grid V061 [Data set] [WWW Document]. NASA EOSDIS Land Process. Distrib. Act. Arch. Cent.

Vetrita, Y., Cochrane, M.A., 2019. Fire frequency and related land-use and land-cover changes in Indonesia's peatlands. Remote Sens. 12, 5.

Vetrita, Y., Cochrane, M.A., Suwarsono, Priyatna, M., Sukowati, K.A.D., Khomarudin, M.R., 2021. Evaluating accuracy of four MODIS-derived burned area products for tropical peatland and non-peatland fires. Environ. Res. Lett. 16, 035015. https://doi.org/10.1088/1748-9326/abd3d1.

World Bank, 2016. The Cost of Fire: An Economic Analysis of Indonesia's 2015 Fire Crisis., Indonesia Sustainable Landscapes Knowledge Note: 1. The World Bank.

Woźniak, E., Aleksandrowicz, S., 2019. Self-adjusting thresholding for burnt area detection based on optical images. Remote Sens. 11, 2669.

Yuwati, T.W., Rachmanadi, D., Pratiwi, Turjaman, M., Indrajaya, Y., Nugroho, H.Y.S.H., Qirom, M.A., Narendra, B.H., Winarno, B., Lestari, S., Santosa, P.B., Adi, R.N., Savitri, E., Putra, P.B., Wahyuningtyas, R.S., Prayudyaningsih, R., Halwany, W., Nasrul, B., Bastoni, Mendham, D., 2021. Restoration of Degraded Tropical Peatland in Indonesia: A Review. Land 10, 1170. https://doi.org/10.3390/land10111170.